Study of Solvent Diffusion in Polymeric Materials Using Magnetic Resonance Imaging

Monique Ercken, Peter Adriaensens, Dirk Vanderzande, and Jan Gelan*

Limburg University, Instituut voor Materiaalonderzoek (IMO), Departement SBG, Universitaire Campus, Gebouw D, B-3590 Diepenbeek, Belgium

Received April 7, 1995; Revised Manuscript Received July 12, 1995[⊗]

ABSTRACT: Magnetic resonance imaging (MRI) has been used to study the diffusion of 1,4-dioxane in poly(vinyl chloride) (PVC) and of acetone (or mixtures of acetone/methanol) in polycarbonate (PC). The results reveal that the system PVC/1,4-dioxane follows the classical Case II theory. The other two systems investigated (PC/acetone and PC with acetone/methanol mixtures) obey Fick's law. In this case, a solvent-induced crystallization takes place after the diffusion front which, at the final stage, leads to a solvent-induced cracking of the material.

Introduction

Polymers in many different applications are exposed to a variety of chemical environments during their lifetime. The presence of, for example, liquids in polymeric materials can have an unwanted effect on their physical properties such as tensile strength and fatigue resistance. Moreover, physical changes to the state of the polymer can occur due to the presence of solvent molecules (e.g., swelling, plasticization, and induced crystallization[1,2]). The diffusion of solvents in polymeric systems covers a wide variety of transport regimes, depending primarily on the nature of the polymer[3,4] and to a lesser extent on the diffusing species.[5,6] The specific features observed during the diffusion process vary greatly depending on whether the polymer is in the rubbery, glassy, or semicrystalline state at the imposed conditions of temperature and pressure.[7] Also the presence of additives[8] (plasticizers, antioxidants, thermal stabilizers, etc.) can modify the state of the polymer at the molecular level and influence the transport properties of the material.

Polymer–solvent systems exhibit a wide range of diffusion phenomena, going from common Fickian diffusion to Case II diffusion.[6,9,10,18] These diffusion characteristics represent the extreme responses of polymers to the solvent and have substantially different characteristics. Fickian (or Case I) diffusion is characterized by an increase in solvent concentration going from the inside of the polymer to the fully swollen regions at the outside of the sample, for which the rate of diffusion is much less than that of the segmental polymer relaxation rates. The distance diffused by a species is proportional to the square root of time and the T_2 relaxation rate is constant throughout the swollen part. This commonly applies to rubbery polymers. Case II behavior on the other hand has the following characteristics: (1) A sharp concentration boundary between the polymer core and the swollen region of the sample is present. (2) The concentration throughout the swollen region is constant. (3) The front advances through the glass at constant velocity. (4) The T_2 relaxation rate decreases toward the polymer core. This behavior is also being called relaxation controlled, because the diffusion is much faster than that of polymer segmental relaxation. This commonly applies to polymers in the glassy state.

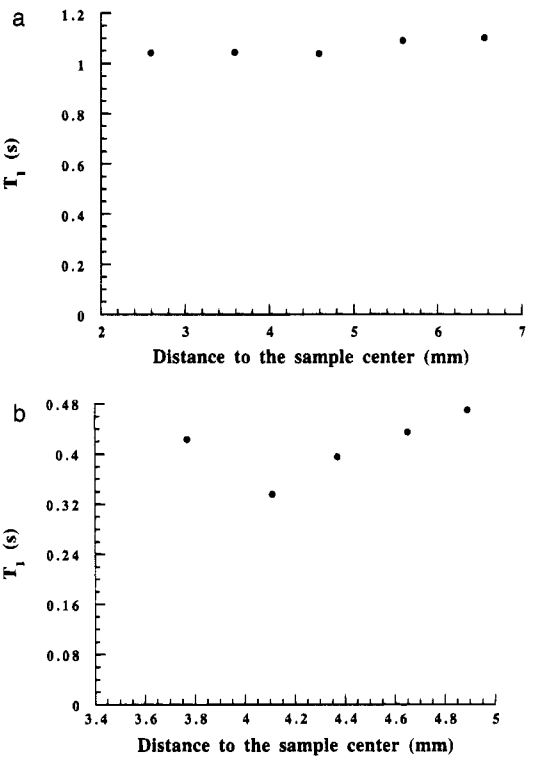

Figure 1. Reconstructed profiles of the T_1 relaxation time of (a) 1,4-dioxane in PVC and (b) acetone in PC. The position 0 on the x-axis is the center of the polymer sample.

Magnetic resonance imaging (MRI) has been established as a method to monitor the diffusion of penetrants into polymers in a nondestructive and noninvasive manner.[11–20] In addition to other techniques, it offers the possibility to look at the spatial solvent molecular mobility by means of the relaxation parameters T_1 and T_2, providing additional evidence toward the type of diffusion. Although other techniques like weight gain measurements can be used to determine the sorption of solvents into a material,[21–23] these techniques mostly demand interruption of the diffusion process and often do not provide information about the spatial distribution of diluent in the polymer nor about the molecular mobility of the penetrated solvent.

In this contribution, the diffusion of 1,4-dioxane in poly(vinyl chloride) (PVC) will be described as a first classical case. As a second system, the diffusion of acetone and mixtures of acetone/methanol in a low molecular weight Bisphenol-A polycarbonate (PC) will

[⊗] Abstract published in *Advance ACS Abstracts,* November 1, 1995.

0024-9297/95/2228-8541$09.00/0

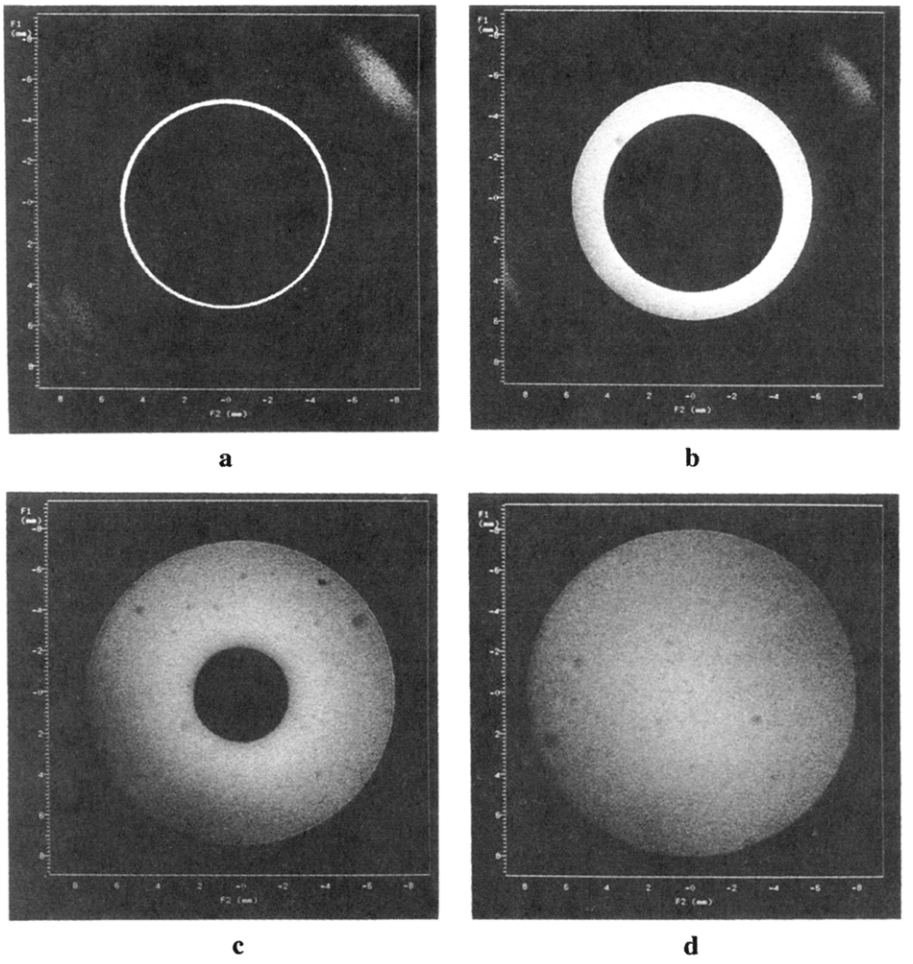

Figure 2. Time-resolved inversion–recovery MRI images (TE = 7 ms, TR = 1 s, TI = 0.566 s) of the diffusion of 1,4-dioxane in a PVC rod (ϕ = 10 mm and height = 25 mm) after (a) 2 h 43 min, (b) 19 h 8 min, (c) 129 h 32 min, or approximately 5 days, and (d) 247 h 39 min, or approximately 10 days.

be investigated. Since these polymers are in the glassy state, one would expect transport characteristics obeying the laws of Case II transport. We want, however, to point out that those classical laws are only valid if no other phase transitions of the polymer than from the glassy to the rubbery state (e.g., solvent-induced crystallization) occur during the diffusion process. As an example, the diffusion of acetone into PC is considered.

Experimental Section

A Bisphenol-A polycarbonate (PC, CT307910) rod with a diameter of 10.7 mm and an unplasticized poly(vinyl chloride) (PVC, CV317910) rod with a diameter of 10 mm were purchased from Goodfellow Cambridge Limited, England. The acetone, methanol, and 1,4-dioxane (all p.a. grade) were purchased from Janssen Chimica.

Time-resolved MRI images of the diffusion process in the polymer matrix were generated at 9.4 T using a Unity 400 Varian spectrometer equipped with a microimaging probe permitting a maximum sample size of 25 mm in diameter. Since the solvents were continuously surrounding the polymer samples, the diffusion process was never interrupted. All the images have an in-plane pixel resolution of about 70 × 70 μm in a field of view of 25 × 25 mm. Slices of 4 mm in thickness were selected in the middle of the specimen. Moreover, a Teflon stopper was placed on top of the rods to avoid longitudinal solvent diffusion. The rods, 10 and 25 mm in length for PC and PVC, respectively, were laid along the direction of the main magnetic field (z-direction) so that radial diffusion into the rods (xy-plane) could be imaged. A common spin-warp sequence with a repetition time TR of 1 s and a spin-echo time TE of 7 ms was used. The surrounding solvent, having a different T_1 relaxation time than the imbibed solvent, was suppressed by using the inversion–recovery method (the inversion time TI was 0.566 s for the PVC/1,4-dioxane system and 0.587 s for PC/acetone). This eliminates problems due to a difference in dynamic range between the intensity of the free solvent compared to the imbibed solvent, allowing a more accurate measurement of the diffusion distance and a higher receiver gain setting. All experiments were made at 16.5 ± 0.5 °C. Furthermore, the diffusion of a mixture acetone/fully deuterated methanol (90/10) was evaluated by the same procedure.

To see whether methanol diffuses along with the acetone into PC or not, the diffusion of an acetone/methanol mixture (70/30) was studied by means of chemical shift selective imaging (CSSI) using a selective Gaussian-shaped pulse. These images were obtained in a sealed NMR-tube without surrounding solvent, since both free acetone and methanol could not be suppressed by a single inversion time.

Since the penetrant swells the polymer, the distance covered by the penetrant or moved by the penetration front was calculated based on the unswollen dimensions of the sample.

$$\text{diffusion distance} = \frac{\text{original sample diameter} - c}{2} \tag{1}$$

where the diameter of the unswollen sample is 10 mm for the PVC rod and 10.7 mm for the PC rod and c (measured on the images) is the diameter of the remaining core.

The spin density (M_0) and T_2 relaxation time of the imbibed solvent as a function of the distance to the core were calculated according to eq 2 by collecting images as a function of TE with fixed TR on partially swollen samples.

$$M = M_0 \exp(-\mathrm{TE}/T_2) \quad (2)$$

These measurements were accomplished without suppressing the surrounding solvent, because this would also alter the imbibed solvent intensity. The M_0 and T_2 values of a certain location were calculated by integrating the intensity M in a small square with fixed coordinates (manually taken) as a function of TE. This was repeated for several locations from the edge of the polymer toward the core. Each integration was averaged over the two opposite directions. To obtain quantitative M_0 values, one has to respect a certain delay time TR ≥ 5 × the T_1 relaxation time at each location measured. The reference T_1 relaxation time of the imbibed solvent was established spectroscopically on a saturated sample using a standard inversion–recovery method. No polymer signal was detected due to severe dipolar broadening in the rigid solid. It was 1.8 and 0.5 s for the PVC/1,4-dioxane and PC/acetone system, respectively. TR used is 9 s for the system PVC/1,4-dioxane and 5 s for the system PC/acetone.

The T_1 of the imbibed solvent as a function of the distance to the core was also calculated by collecting images as a function of TR with TE constant on partially swollen samples. It was noticed that T_1 slightly decreases toward the core in the case of the system PVC/1,4-dioxane (Figure 1a) and that these values were smaller than T_1 measured spectroscopically. Indeed, the solvent mobility will be the highest for saturated samples since no restrictions on the solvent mobility due to the glassy core remain. Since solvent mobility, in general, is situated in the extreme narrowing range (situated at higher mobility with respect to the T_1 minimum), the longest T_1 relaxation time will occur for the highest solvent mobility. For the system PC/acetone (Figure 1b), a TR of even 10 times T_1 was used.

The thermal behavior of the polycarbonate was studied by differential scanning calorimetry (DSC), using a DuPont 910 differential scanning calorimeter.

Results and Discussion

Diffusion of 1,4-Dioxane in Poly(vinyl chloride). Images of the time-resolved diffusion of 1,4-dioxane in a PVC rod (dimensions 10 × 25 mm) are presented in Figure 2. The surrounding solvent, having a different T_1 relaxation time than the imbibed solvent, is suppressed by the inversion–recovery technique. Two different processes can clearly be observed: solvent penetration into the rod and polymer swelling. Figure 3 shows a plot of the diffusion distance (corrected for the swelling of the matrix) of 1,4-dioxane into PVC as a function of time. Fitting these results gives a time dependence of $t^{0.91}$. This almost linear front advance is typical for the diffusion of solvents into a glassy polymer (=Case II diffusion).[10,11,20] Another requirement for Case II transport is that the dry polymer exists initially in a glassy state and that the penetrating solvent is capable of lowering the glass transition temperature T_g.[24] PVC, swollen in 1,4-dioxane, clearly exists in the rubbery state. Figure 4 presents the swelling of the sample diameter during the diffusion process as a function of square root of time. This swelling ratio was defined as follows:

$$\%\ \text{swelling} = \frac{D(t) - D_0}{D_0} \times 100 \quad (3)$$

where $D(t)$ is the sample diameter at time t and D_0 is the initial diameter. A linear dependence with square root of time can be clearly noticed. This seems to indicate that the swelling obeys Fick's law, which is assigned to polymers in the rubbery state.[18] The onset, observed at short exposure times, reflects the polymer equilibration starting the process of diffusion.[25] Clearly,

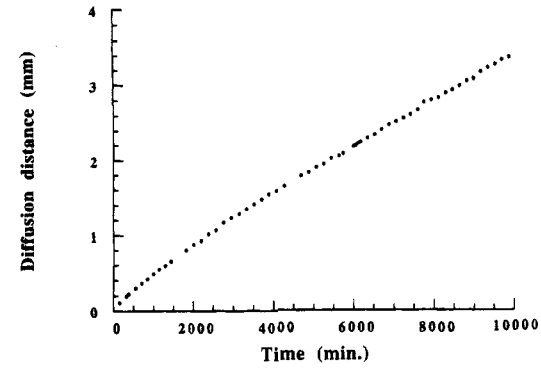

Figure 3. Diffusion distance of 1,4-dioxane into PVC versus time.

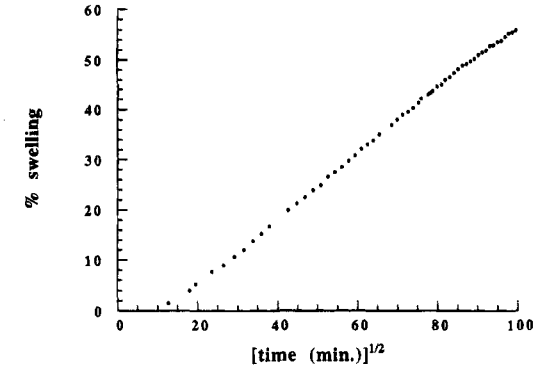

Figure 4. Swelling behavior of a PVC rod in 1,4-dioxane as a function of square root of time.

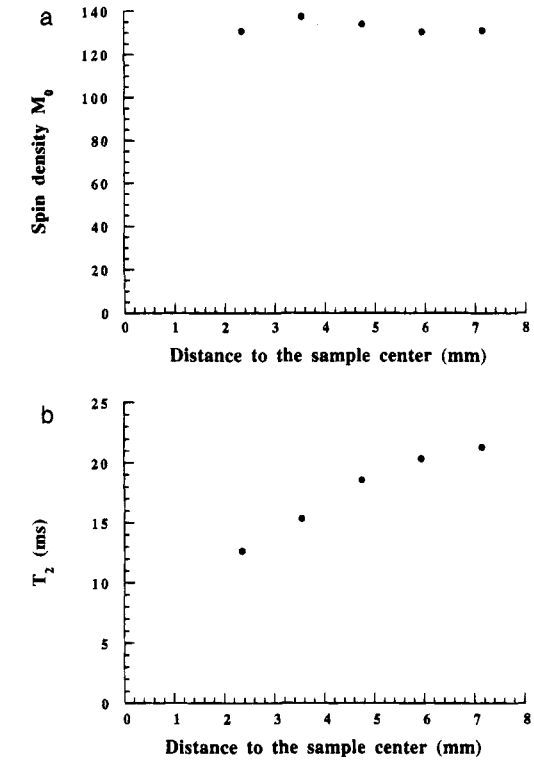

Figure 5. Reconstructed profiles of (a) the spin density M_0 and (b) the solvent mobility T_2 of 1,4-dioxane in PVC. The position 0 on the x-axis is the center of the polymer sample. Notice the swelling of the sample to a diameter of about 14 mm.

the swelling of the polymer and the solvent diffusion into the glassy core are two distinct processes. Solvent-induced dilation of a macromolecular polymeric system in the glassy and/or the rubbery state results from

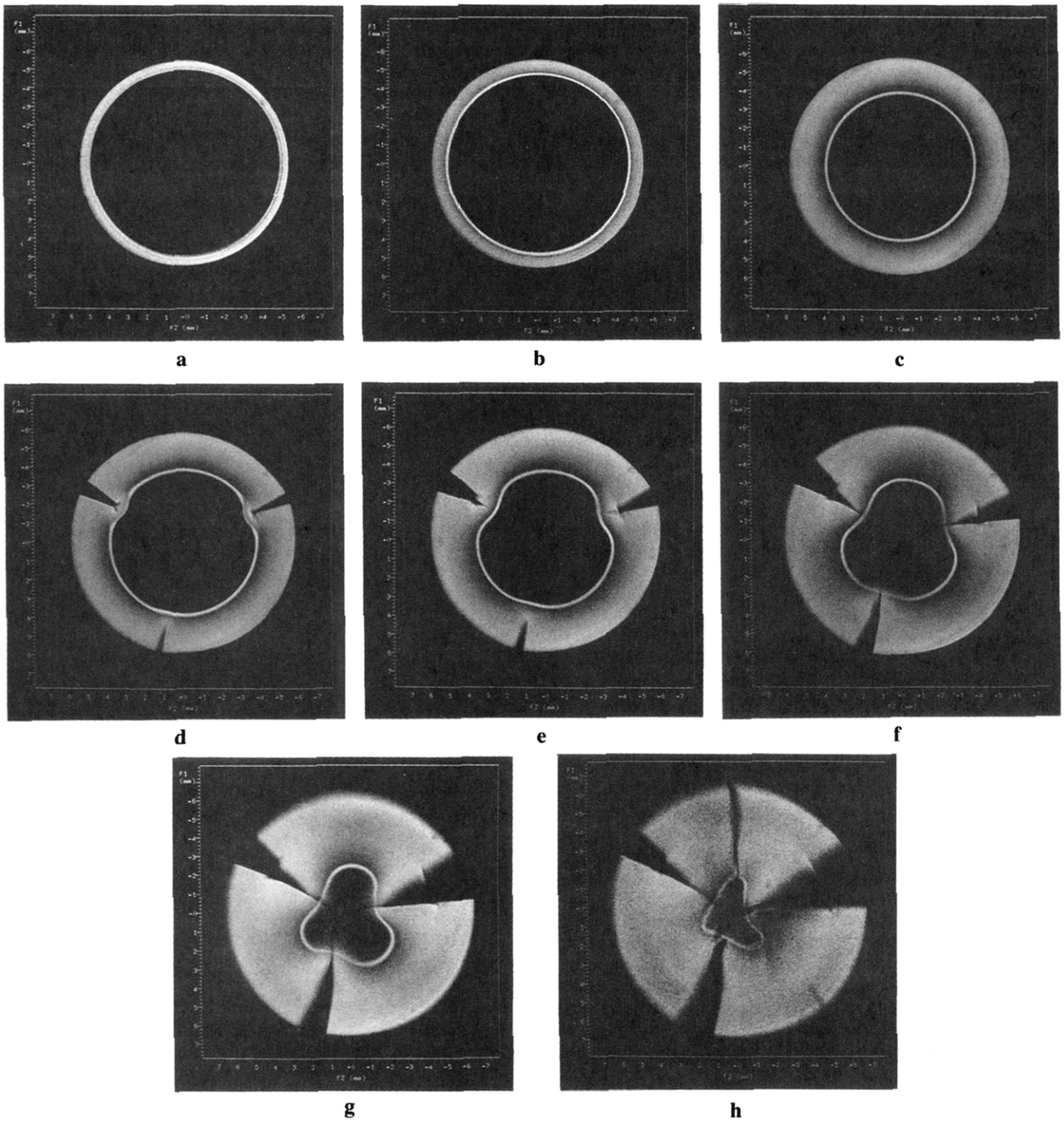

Figure 6. Time-resolved inversion–recovery MRI images (TE = 7 ms, TR = 1 s, TI = 0.587 s) of the diffusion of acetone in a polycarbonate rod (ϕ = 10.7 mm and height = 10 mm) after (a) 1 h 0min, (b) 2 h 50 min, (c) 19 h 29 min, (d) 21 h 25 min, (e) 28 h 12 min, (f) 46 h 47 min, (g) 61 h 23 min, and (h) 74 h 53 min.

osmotic stresses opposite to a restraining force.[26] Kinetically, the character of transport, hence dilation, is different in the two states. In Case II transport, the penetrant enters the glassy matrix faster than the polymer can adapt itself by volume relaxation. Due to the softening of the material behind the diffusion front, the polymer relaxation in the already swollen matrix is fast enough to adapt to a new situation created by further solvent uptake. Therefore, solvent ingress as well as swelling behind the diffusion front will be Fickian.

NMR relaxation parameters are a useful probe for molecular motions in polymers and other organic molecules.[11,27–30] MRI permits the determination of the spatial distribution of NMR relaxation times.[19,31–33] This distribution provides information concerning the homogeneity of local motions in the system. According to eq 2, one can simultaneously monitor the spatial distribution of the T_2 parameter and the spin density M_0, which represents the solvent concentration in the polymer. These profiles have been reconstructed for 1,4-dioxane in PVC. The sample was already considerably swollen. The volume fraction of 1,4-dioxane in the polymer, shown in Figure 5a, is constant from the polymer surface to the glassy core. In contrast, the T_2 values change substantially from the surface to the core (Figure

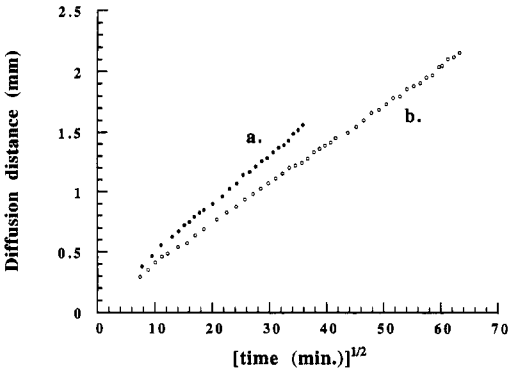

Figure 7. Diffusion distance of (a) acetone and (b) the mixture acetone/deuterated methanol (90/10) into PC versus square root of time.

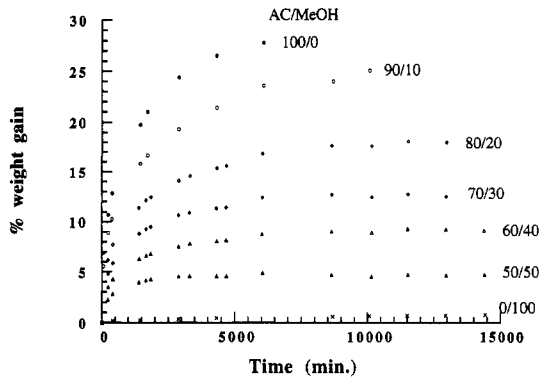

Figure 8. Percent weight gain versus time for various mixtures of acetone/methanol diffusing into PC.

5b), showing that the glassy polymer core reduces the chain mobility in the swollen area from the outside toward the glassy region of the polymer. So, the polymer chain dynamics change from the usual isotropic motions with a variety of frequencies and amplitudes to anisotropic motions with frequencies and amplitudes dependent on the position relative to the front of the glassy core. These findings confirm the Case II transport mechanism.[19]

Acetone and Acetone/Methanol Mixtures in Polycarbonate. Figure 6 shows some images of the time course of acetone diffusion into a PC rod (dimensions 10.7 × 10 mm). The surrounding solvent, having a different T_1 relaxation time than the imbibed solvent, is suppressed by the inversion–recovery technique. In Figure 6a, the formation of a high-intensity ring around the core can be noticed, which becomes more clear in time. When the solvent proceeds into the PC rod, a darkening from the outer side towards the white ring can be seen (Figure 6c). After approximately 21 h, the rod suddenly cracks in the imbibed region. At the tip of the crack, the white ring is pushed further into the core, while the cracking goes on (Figure 6e–h). In Figure 6g, one can clearly see the cracks having reached the center of the core. Similar images were obtained by imaging the acetone diffusion of a mixture of acetone/deuterated methanol (90/10 on a volumetric basis). Comparable to the pure acetone case, also here a bright zone appears around the core and the polymer cracks over the course of time, although the cracking occurs later (after 69 h instead of 21 h).

The movement of the solvent fronts (corrected for the minor swelling according to equation 1) of pure acetone and acetone in the 90/10 mixture into PC versus square root of time is shown in Figure 7. The end of the curve coincides with the cracking of the rod. Apparently, there is a linear dependence between the diffusion distance and the square root of time. This indicates that the diffusion is Fickian, which is in good agreement with results reported by others.[15,34–36] This may seem contrary to what is usually found for the diffusion of solvents into a glassy polymer. Instead, either Case II or anomalous diffusion is most often encountered at temperatures far below the T_g of the pure thermoplast.[10,26,37] The diffusion of acetone in the 90/10 mixture is slower compared to the diffusion of pure acetone. Initial experiments involved the analysis of simple weight gain measurements for a variety of acetone/methanol mixtures. Percent weight gain (determined analogously to eq 3) versus time for various mixtures of acetone/methanol are plotted in Figure 8. It can be seen that pure acetone diffuses and saturates PC rather quickly and that the saturation content of the mixtures decreases with increasing methanol content. This can be supported by the polymer–solvent interaction parameter, χ, of 2.06 for the system PC–methanol.[35] It is generally accepted that when the value of χ exceeds 0.5, no favorable interaction between the solvent and the polymer exists. This is in contrast to a χ-value of 0.36 for the PC–acetone system.

To check whether the methanol diffuses along with the acetone, a PC rod was immersed in an acetone/methanol mixture (70/30) for approximately 1 week. It must be mentioned that the polymer matrix did not crack over this time period. The chemical shift selective images of acetone and the methyl resonance of methanol are shown in Figures 9a and b, respectively. In spite of the higher acetone concentration in the mixture, the higher acetone concentration in the polymer (acetone is a better solvent for PC than methanol) and the higher proton count in acetone, the acetone image is rather noisy compared to the methanol image. Since the image is acquired without surrounding solvent (see Experimental Section), it is due to the evaporation of the acetone during the experiment. Though methanol is a poor solvent for PC (χ = 2.06), it is clearly present (Figure 9b). Also notice that the white ring around the core is obviously somewhat broader. It may be proposed[38] that the good solvent (here acetone) is enhancing the accessibility of the poor solvent (here methanol), while the methanol is depressing the accessibility of acetone.

According to eq 2, the spin density (M_0) and the T_2 relaxation time of the pure acetone as a function of the distance to the core have been calculated. The volume fraction of acetone in PC, shown in Figure 10a, decreases from the polymer surface toward the white ring around the core, while the solvent mobility (T_2) remains constant throughout the imbibed region (Figure 10b). In contrast, a sudden increase of the solvent concentration and mobility can be observed in the white ring. Also notice the sudden increase in T_1 (increase of solvent mobility) in the white ring in Figure 1b. Except for the white ring, these findings confirm an apparent Fickian diffusion process. A constant solvent mobility in the imbibed region means that the unaffected glassy core in the polymer matrix does not influence the polymer chain dynamics in this region.

Concerning the cracking of the PC rod, it was noticed that the diffusion of acetone into PC causes opacity to develop in the polymer as a result of crystallization. In the DSC thermogram of the amorphous PC, only a glass transition temperature T_g around 160 °C can be observed (Figure 11a). The DSC thermogram of the PC

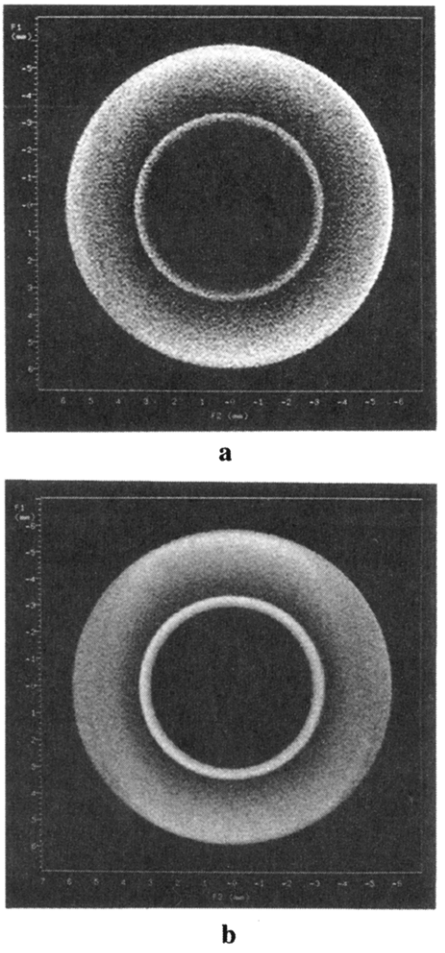

Figure 9. Chemical shift selective images of (a) acetone and (b) methanol in a PC rod immersed approximately 1 week in a 70/30 acetone/methanol mixture.

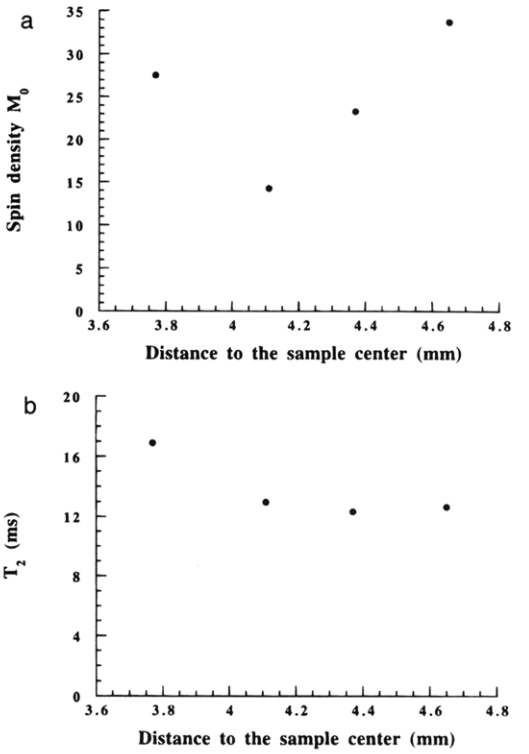

Figure 10. Reconstructed profiles of (a) the spin density M_0 and (b) the solvent mobility T_2 of acetone in PC. The position 0 on the x-axis is the center of the polymer sample.

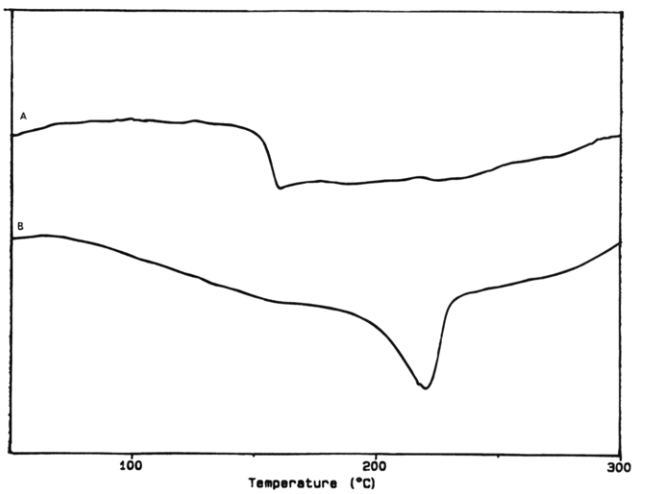

Figure 11. DSC thermogram of (a) the amorphous PC ($T_g \sim$ 160 °C) and of (b) the PC after the acetone diffusion ($T_m \sim$ 220 °C).

after the diffusion process (Figure 11b) shows an additional melting endotherm around 220 °C. PC is a polymer which is difficult to crystallize and is normally produced in its amorphous form. At 190 °C, 1 day is necessary for the first crystallites to develop and at least 1 week to obtain a crystalline material with a well-developed spherulitic structure.[41] The difficulty in crystallizing PC by thermal annealing despite its regular structure has been attributed to the small temperature range between the melting point T_m (±265 °C) and the T_g (±150 °C) of the pure polymer.[35] The crystallization, however, of some polymers (e.g., PC) is facilitated by the presence of organic vapors and liquids.[7,8,34-36,39-41] Thus, when acetone enters and softens the PC, it increases the mobility of the polymeric segments (T_g is depressed), allowing a reorientation of the polymer chains. Under these circumstances, T_g will be depressed to a larger extent than T_m, widening the temperature gap between T_m and T_g. Makarewicz and Wilkes[42] have shown that a 50% increase in the gap between T_m and T_g for PET can result in a tenfold increase in the polymer crystallization rate. This ordering of the polymer chains creates shearing forces due to a decrease of free volume, causing the environmental stress cracking (ESC).

By examining Figure 6 carefully, the following details are to be distinguished: the unaffected sample core (dark), a high-intensity white ring, and the imbibed region. Turska and Benecki[39] also observed a separate region behind the diffusion front using microscopy. They explained it as a distinct separation between the diffusion and crystallization fronts. It must be noticed that the polycarbonate does not immediately crystallize just behind the diffusion front, where the polymer matrix is already sufficiently swollen for the crystallization process to take place. This can be explained by a crystallization induction period, analogous to that found for the thermal crystallization of polycarbonate,[43] demonstrated by the experiments of Turska and Benecki.[39]

Concerning Figure 10, one can see that the mobility (T_2) and solvent concentration are much higher in the white ring than in the imbibed region. These are the features of a highly swollen zone. During the crystallization process, solvent is rejected out of the crystallizing region, due to a decrease in free volume. This allows the acetone to penetrate into the PC at a higher rate, so a deviation from the normal Case II diffusion

toward an apparent Fickian diffusion process takes place. It also explains the high solvent concentration in the white ring and the rather low concentration immediately behind the white ring. The increase in concentration toward the polymer surface can be interpreted as the driving force of the system to establish a state of equilibrium, where the restraining force of the polymer equals the osmotic pressure. Since stress cracking of PC is due to an acetone-induced reorientation of the polymer chains, it can be slowed down by diluting the cracking agent, as was demonstrated for the acetone diffusion in the 90/10 mixture (Figure 7b). Due to a delayed crystallization (cracking) and diffusion, the width of the swollen region clearly increases upon acetone dilution (see Figure 9 for the 70/30 mixture).

Conclusion

The system poly(vinyl chloride)/1,4-dioxane clearly follows the classical Case II theory, which is normal for the diffusion of solvents into glassy polymers. A linear uptake of 1,4-dioxane with time, a constant solvent concentration through the imbibed region, and a decreasing solvent mobility (T_2) toward the glassy core can be observed. On the other hand, attention has to be paid, in general, when studying the diffusion of solvents in polymeric materials. Following the diffusion of acetone and acetone/methanol mixtures in polycarbonate, apparently a Fickian diffusion takes place. There is a linear dependence between front movement and square root of time, the solvent concentration decreases toward the glassy core, and the solvent mobility (T_2) remains constant. These are all characteristic for Fickian diffusion. A solvent-induced crystallization process, however, creates high shearing forces and a decrease of free volume, pushing the solvent in a high-intensity area (white ring) around the glassy core and forcing it to penetrate more rapidly into the core.

Acknowledgment. We are grateful to the IWT (Flemish Institute for the Promotion of Scientific Technological Research) for financial support of this research. The authors thank Prof. Dr. H. Berghmans (K. U. Leuven) for his valuable comments.

References and Notes

(1) Deberdt, F.; Berghmans, H. *Polymer* **1994**, *35*, 1694.
(2) Overbergh, N.; Berghmans, H.; Smets, G. *Polymer* **1975**, *16*, 703.
(3) Naylor, T. *Comprehensive Polymer Science*; Pergamon Press: Oxford, 1989; Vol. 2, Chapter 20.
(4) Stern, S. A.; Shah, V. M.; Hardy, B. J. *J. Polym. Sci., Polym. Phys. Ed.* **1987**, *25*, 1293.
(5) Markin, V. S.; Zaikov, G. E. *Polym. Degrad. Stab.* **1993**, *40*, 395.
(6) Frisch, H. L. *Polym. Eng. Sci.* **1980**, *20*, 2.
(7) Crank, J.; Park, G. S. *Diffusion in Polymers*; Academic Press: New York, 1968.
(8) Markin, V. S.; Zaikov, G. E. *Polym. Degrad. Stab.* **1993**, *40*, 389.
(9) Vrentas, J. S.; Duda, J. L.; Huang, W. J. *Macromolecules* **1993**, *26*, 1841.
(10) Alfrey, T.; Gurnee, E. F.; Lloyd, W. G. *J. Polym. Sci., Part C: Polym. Lett.* **1966**, *12*, 249.
(11) Ilg, M.; Pfleiderer, B.; Albert, K.; Rapp, W.; Bayer, E. *Macromolecules* **1994**, *27*, 2778.
(12) Perry, K. L.; McDonald, P. J.; Clough, A. S. *Magn. Reson. Imaging* **1994**, *12*, 217.
(13) Perry, K. L.; McDonald, P. J.; Randall, E. W.; Zick, K. *Polymer* **1994**, *35*, 2744.
(14) Komoroski, R. A. *Anal. Chem.* **1993**, *65*, 1068A.
(15) Grinsted, R. A.; Koenig, J. L. *Macromolecules* **1992**, *25*, 1229.
(16) Maffei, P.; Kiéné, L.; Canet, D. *Macromolecules* **1992**, *25*, 7114.
(17) Grinsted, R. A.; Clark, L.; Koenig, J. L. *Macromolecules* **1992**, *25*, 1235.
(18) Webb, A. G.; Hall, L. D. *Polymer* **1991**, *32*, 2926.
(19) Weisenberger, L. A.; Koenig, J. L. *Macromolecules* **1990**, *23*, 2445.
(20) Weisenberger, L. A.; Koenig, J. L. *Appl. Spectrosc.* **1989**, *43*, 1117.
(21) Arzak, A.; Eguiazabal, J. I.; Nazabal, J. *J. Mater. Sci.* **1993**, *28*, 3272.
(22) Aminabhavi, T. M.; Munnolli, R. S. *Polym. Int.* **1993**, *32*, 61.
(23) Aminabhavi, T. M.; Khinnavar, R. S. *Polymer* **1993**, *34*, 1006.
(24) Cody, G. D.; Botto, R. E. *Macromolecules* **1994**, *27*, 2607.
(25) Roussel, J. C.; Serpe, G.; Gautier, S.; Rodgers, P. *J. Chim. Phys.* **1994**, *91*, 704.
(26) Thomas, N. L.; Windle, A. H. *Polymer* **1982**, *23*, 529.
(27) Zhang, X.; Solomon, D. H. *Macromolecules* **1994**, *27*, 4919.
(28) Shaohua, H.; Masaki, T.; Fumitaka, H. *Polymer* **1994**, *35*, 2516.
(29) Bayer, E.; Albert, K.; Willisch, H.; Rapp, W.; Hemmasi, B. *Macromolecules* **1990**, *23*, 1937.
(30) Voelkel, R. *Angew. Chem., Int. Ed. Engl.* **1988**, *27*, 1468.
(31) Rana, M. A.; Koenig, J. L. *Macromolecules* **1994**, *27*, 3727.
(32) Smith, S. R.; Koenig, J. L. *Macromolecules* **1991**, *24*, 3496.
(33) Clough, R. S.; Koenig, J. L. *J. Polym. Sci., Part C: Polym. Lett.* **1989**, *27*, 451.
(34) Miller, G. W.; Visser, S. A. D.; Morecroft, A. S. *Polym. Eng. Sci.* **1971**, *11*, 73.
(35) Ware, R. A.; Tirtowidjojo, S.; Cohen, C. *J. Appl. Polym. Sci.* **1981**, *26*, 2975.
(36) Turska, E.; Benecki, W. *J. Polym. Sci.* **1974**, *44*, 59.
(37) Hui, C.-Y.; Wu, K.-C.; Lasky, R. C.; Kramer, E. J. *J. Appl. Phys.* **1987**, *61*, 5129.
(38) Vahdat, N. *J. Appl. Polym. Sci.* **1993**, *50*, 1833.
(39) Turska, E.; Benecki, W. *J. Appl. Polym. Sci.* **1979**, *23*, 3488.
(40) Wilkes, G. L. *Polym. Prepr. (Am. Chem. Soc., Div. Polym. Chem.)* **1976**, *17*, 937.
(41) Mercier, J. P.; Groeninckx, G.; Lesne, M. *J. Polym. Sci., Part C* **1967**, *16*, 2059.
(42) Makarewicz, P. J.; Wilkes, G. L. *J. Polym. Sci., Polym. Phys. Ed.* **1969**, *7*, 2019.
(43) Von Falkai, B. V.; Rellensman, W. *Makromol. Chem.* **1965**, *88*, 38.

MA950484X